
A Biological Method to Evaluate Bifunctional Chelating Agents to Label Antibodies with Metallic Radionuclides

Yasushi Arano, Takahiro Mukai, Takashi Uezono, Kouji Wakisaka, Hiroshi Motonari, Hiromichi Akizawa, Yuuko Taoka and Akira Yokoyama

Faculty of Pharmaceutical Sciences, Kyoto University, Sakyo-ku, Kyoto, Japan

Since the lysosome is a common organelle for protein digestion, pursuing the fate of radiolabeled metabolites after lysosomal proteolysis in liver cells is ideal to evaluate bifunctional chelating agents (BCAs). **Methods:** We used galactosyl-neoglycoalbumin (NGA) and mannosyl-neoglycoalbumin (NMA) as carrier proteins for hepatic parenchymal and nonparenchymal cells, respectively. These proteins were labeled with ^{111}In using 1-(4-isothiocyanatobenzyl)ethylenediaminetetraacetic acid (SCN-Bz-EDTA) as a model. **Results:** NGA-SCN-Bz-EDTA- ^{111}In exhibited rapid accumulation in the hepatic parenchymal cells, followed by hepatobiliary excretion of the metabolites with an elimination rate that was faster and much slower than that of NGA-DTPA- ^{111}In and NGA- ^{131}I , respectively. This metabolite represented all the radioactivity registered in the liver at 1 hr postinjection. Subcellular distribution studies indicated the metabolites were located only in the lysosome fraction, and the difference in elimination rates of the metabolites from the lysosome fraction was responsible for the variations in radioactivity clearance from the cells. **Conclusion:** The biological characteristics of radiolabeled metabolites play a critical role in eliminating the radiolabel from liver cells. The present method portrays a highly useful model to pursue the fate of radiolabeled metabolites in the liver.

Key Words: monoclonal antibodies; indium-111; nontarget radioactivity; neoglycoalbumin; metabolism

J Nucl Med 1994; 35:890–898

In the diagnostic and therapeutic application of monoclonal antibodies (Mabs) labeled with metallic radionuclides, high radioactivity localization in the liver is a major problem. Numerous new bifunctional chelating agents (BCAs) rendering higher in vivo stability of the resulting radiometal chelates have been developed to decrease the undesirable radioactivity localization (1–5). Although some of these new BCAs have demonstrated reduced radioactivity levels in animal livers, high hepatic radioactivity is still visualized

in clinical studies (6). These results suggest that factors other than in vivo instability of the radiometal chelates are also responsible for the hepatic radioactivity localization of Mabs labeled with metallic radionuclides. Furthermore, biodistribution studies of radiolabeled Mabs in animal models may not always coincide with clinical results. Recent studies on the metabolism of ^{111}In -labeled Mabs have shown that their catabolism in the liver is very rapid, and the slow elimination rate of radiolabeled metabolites from the liver is responsible for the prolonged hepatic radioactivity localization (7–9). As such, biological methods that can pursue the fate of radiolabels after hepatic incorporation are highly required for the practical evaluation of radiolabeling agents such as BCAs.

Since lysosomes are the principal sites of intracellular digestion of proteins, peptides (10) and antibodies (11,12), an approach to pursue the fate of radiolabeled metabolites at this organelle after hepatic uptake may be rewarding. For the development of such an experimental system, selection of carrier proteins or peptides that can be incorporated in liver cells and subsequently transported to the lysosomal compartment within a short postinjection time by known mechanisms would be useful to minimize the transchelation and redistribution of radiolabels generated in tissues and fluid outside the liver. In addition, the carrier protein should be conjugated with BCAs in a procedure similar to that of Mabs with BCAs.

Uptake of galactosyl-neoglycoalbumin (NGA) by hepatic parenchymal cells via receptor-mediated endocytosis has been well documented (13–15). After binding at the surface, NGA is rapidly internalized via coated pits and then transported intracellularly to the lysosomal compartment. This process is much faster than the rate at which substrates dissolved in the extracellular fluid enter cells by fluid-phase endocytosis (10). Similar mechanisms have been observed in the incorporation of mannosyl-neoglycoalbumin (NMA) by hepatic nonparenchymal cells (Kupffer cells and endothelial cells) (13,15,16). These biological characteristics render NGA and NMA useful as carrier proteins for estimating the fate of radiolabeled metabolites after lysosomal proteolysis in parenchymal and

Received Aug. 24, 1993; revision accepted Jan. 26, 1994.

For correspondence or reprints contact: Akira Yokoyama, PhD, Dept. of Radio-pharmaceutical Chemistry, Faculty of Pharmaceutical Sciences, Kyoto University, Sakyo-ku, Kyoto 606 Japan.

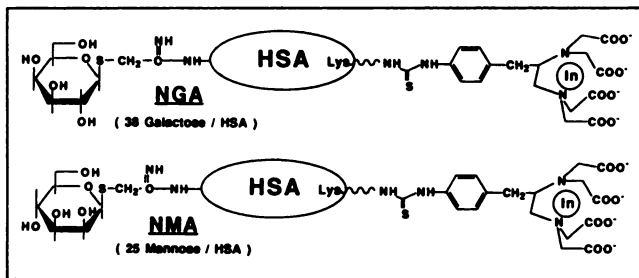


FIGURE 1. Chemical structures of NGA-SCN-Bz-EDTA-¹¹¹In and NMA-SCN-Bz-EDTA-¹¹¹In.

nonparenchymal cells of the liver within a short postinjection time.

In the present study, 1-(4-isothiocyanatobenzyl)ethylenediaminetetraacetic acid (SCN-Bz-EDTA) was used as a model BCA in ¹¹¹In labeling of NGA and NMA. SCN-Bz-EDTA is covalently linked to the ε-amino groups of lysine residues in Mabs, NGA and NMA via the thiourea bond to produce ¹¹¹In chelates with high in vivo stability (Fig. 1) (3, 17). The biodistribution of radioactivity after injection of NGA-SCN-Bz-EDTA-¹¹¹In and NMA-SCN-Bz-EDTA-¹¹¹In in mice was compared with that of ¹¹¹In-DTPA- and ¹³¹I-labeled neoglycoalbumins to study the elimination routes and rates of the radiolabels from each liver cell type. Furthermore, the chemical forms of radiolabeled metabolites remaining in the liver and excreted from the body, and subcellular localization of radiolabeled metabolites in the liver were investigated after intravenous injections of NGA- and NMA-SCN-Bz-EDTA-¹¹¹In in mice. This approach provided insight into the metabolism of SCN-Bz-EDTA-¹¹¹In-conjugated proteins in liver.

MATERIALS AND METHODS

NGA-SCN-Bz-EDTA-¹¹¹In and NMA-SCN-Bz-EDTA-¹¹¹In

Cyanomethyl-2,3,4,6-tetra-O-acetyl-1-thio-β-D-galactopyranoside and cyanomethyl-2,3,4,6-tetra-O-acetyl-1-thio-β-D-mannopyranoside were synthesized according to the procedure of Lee et al. (18). These compounds were conjugated with human serum albumin (HSA; A-3782, Sigma Chemical Co., St. Louis, MO), according to the procedure of Stowell et al. (19). When determined with the TNBS method (20), 38 galactoses and 25 mannoses were attached to each molecule of HSA backbone for NGA and NMA, respectively.

NGA-SCN-Bz-EDTA and NMA-SCN-Bz-EDTA were prepared by adding 10 molar excess of 1-(4-isothiocyanatobenzyl)ethylenediaminetetraacetic acid (SCN-Bz-EDTA; Dojindo Labs, Kumamoto, Japan) in dimethylformamide (7.3 mg/ml) to NGA or NMA (10 mg/ml) in borate-buffered saline (0.05 M, pH 8.5) prior to incubation at 37°C for 20 hr. Both conjugates were then purified by Sephadex G-50 (Pharmacia Biotech Co. Ltd., Tokyo, Japan) column chromatography (1.8 × 40 cm) equilibrated and eluted with 0.1 M acetate buffer (pH 3.0) or with 20 mM of 2-(N-morpholino)ethanesulfonic acid (MES) buffered saline (pH 6.0). The respective conjugate fractions collected were subsequently concentrated to 5 mg/ml by ultrafiltration (8 MC model, Amicon Grace, Tokyo, Japan).

Lysine-SCN-Bz-EDTA was synthesized by reacting *t*-butoxy-

carbonyl-L-lysine (Boc-L-lysine; Kokusan Chemical Works, Ltd., Tokyo, Japan) with SCN-Bz-EDTA in a H₂O-to-pyridine mixture (1:9) followed by treatment with trifluoroacetic acid to remove the Boc group.

NGA- and NMA-SCN-Bz-EDTA were labeled with ¹¹¹In according to the procedure of Brechbiel et al. (1) with slight modification. Briefly, 4 μl of HCl (1.75 N) and 16 μl of sodium acetate (1 M) were added to 20 μl of ¹¹¹InCl₃ in 0.01 N HCl (2 mCi/ml). A volume of 20–40 μl of the ¹¹¹In solution was added to 200 μl (5 mg/ml) of either NGA-SCN-Bz-EDTA or NMA-SCN-Bz-EDTA in 20 mM MES-buffered saline (pH 6.0). The mixture was stirred gently for 1 hr at room temperature. NGA- and NMA-SCN-Bz-EDTA were also labeled with ¹¹¹In by the addition of ¹¹¹InCl₃ (2 mCi/ml, 10–200 μl) to either NGA-SCN-Bz-EDTA or NMA-SCN-Bz-EDTA (5 mg/ml, 100 μl) in 0.1 M acetate buffer (pH 3.0). The reaction mixture was agitated gently for 1.5 hr at room temperature. Lysine-SCN-Bz-EDTA and 1-(4-aminobenzyl)ethylenediaminetetraacetic acid (NH₂-Bz-EDTA, Dojindo Labs) were labeled with ¹¹¹In by adding 10 μl of ¹¹¹In acetate (prepared as described above) to 100 μl of the respective ligand (0.6 mg/ml) in 0.1 M acetate buffer (pH 3.0). The reaction mixture was allowed to stand at room temperature for 10 min.

NGA-DTPA-¹¹¹In and NMA-DTPA-¹¹¹In

To a solution of NGA (10 mg/ml) in borate buffer (0.05 M, pH 8.5), 5 molar excess of cyclic DTPA dianhydride (Dojindo Labs) in dimethylsulfoxide (2.5 mg/ml) was added. After stirring gently for 30 min, NGA-DTPA was purified by Sephadex G-50 column chromatography (1.8 × 40 cm) equilibrated and eluted with citrate buffer (0.1 M, pH 6.0). The conjugate was finally pooled and concentrated to 5 mg/ml by ultrafiltration (8 MC). NMA-DTPA was synthesized in a manner similar to the procedure described above except that NMA was used in place of NGA.

NGA-DTPA and NMA-DTPA were labeled with ¹¹¹In by adding 25 μl of ¹¹¹InCl₃ (50 μCi) in 0.01 N HCl to 100 μl of each conjugate in the citrate buffer. The mixture was allowed to incubate at room temperature for 2 hr.

To evaluate nonspecifically bound ¹¹¹In in each ¹¹¹In-labeled NGA and NMA, 10 mM ethylenediaminetetraacetic acid (EDTA) in 0.1 M of acetate buffer (pH 3.0 or 6.0) was added to each ¹¹¹In-labeled neoglycoalbumin to reach 100 molar excess of EDTA for each protein molecule. After incubating 5 and 60 min at room temperature, the reaction mixture was spotted on silica gel TLC (Merck Art. 5553) developed with 10% ammonium chloride-to-methanol (1:1) and celluloseacetate electrophoresis (CE) run at an electrostatic field of 0.8 mA/cm for 40 min in a veronal buffer (I = 0.05, pH 8.6). The radioactivity in the protein fraction was then determined.

Iodine-131-Labeled NGA and NMA

Radioiodination of both NGA and NMA with Na¹³¹I was achieved by the chloramine-T method (21), followed by purification by Sephadex G.50 column chromatography (0.8 × 17 cm) equilibrated and eluted with phosphate buffer (0.1 M, pH 7.0).

The radiochemical purity of ¹¹¹In- and ¹³¹I-labeled NGA and NMA was determined by TLC, CE and size-exclusion HPLC. TLC and CE analyses were carried out under the conditions as described above and size-exclusion HPLC (5Diol-120, 7.5 × 600 mm, Nacalai Tesque, Kyoto, Japan) was eluted with 0.1 M phosphate buffer (pH 6.8).

In Vivo Studies

The protein concentrations of ^{111}In - and ^{131}I -labeled NGA and NMA were diluted and adjusted with 0.1 M phosphate-buffered saline (PBS, pH 6.0) to 90 $\mu\text{g}/\text{ml}$. Biodistribution studies were investigated by the intravenous injections of respective radiolabeled neoglycoalbumins to 6-wk-old male ddY mice (27–30 g) (22). Groups of five mice each were administered with 9 μg (0.3–0.5 μCi) of the respective labeled proteins prior to death at 10 and 30 min, 1, 3, 6, and 24 hr postinjection by decapitation. Tissues of interest were then removed, weighed and the radioactivity counts were determined (Beckman Co. Ltd., Gamma-5500, Tokyo, Japan).

To assess the cellular localization of radioactivity in murine liver cells, parenchymal and nonparenchymal cells were fractionated by collagenase perfusion *in situ* from the portal vein 15 min after intravenous injection of NGA- and NMA-SCN-Bz-EDTA- ^{111}In with Type I collagenase (C-0130, Sigma Chemical Co.) dissolved in an EDTA-free solution (23).

NGA- and NMA-SCN-Bz-EDTA- ^{111}In were similarly injected into 6-wk-old male ddY mice (9 μg protein/mouse) in the presence of 200 and 400 μg of NGA and NMA, respectively. At 10 min postinjection, animals were decapitated and tissues of interest were removed, weighed and the radioactivity was counted.

To evaluate the behaviors of nonspecifically bound ^{111}In of NGA and NMA, these two proteins were directly labeled with ^{111}In according to the procedures similar to those of NGA- and NMA-SCN-Bz-EDTA- ^{111}In before intravenous administration in mice (9 μg protein/mouse). The radioactivity distribution was examined at 10 min and 24 hr postinjection, accordingly.

To investigate the radiolabeled metabolites, NGA-SCN-Bz-EDTA- ^{111}In and NMA-SCN-Bz-EDTA- ^{111}In (3.6–7.2 $\mu\text{Ci}/9$ μg each) was administered intravenously to 6-wk-old male ddY mice. At 1, 3 and 24 hr postinjection, livers of ether-anesthetized mice were treated according to the method as previously described (24,25). Briefly, the murine liver was perfused *in situ* with cold 0.1 M tris-citrate buffer (pH 6.5) containing 0.15 M NaCl, 0.002% sodium azide, 1 TIU/ml aprotinin, 2 mM benzamide-HCl, 2 mM iodoacetamide and 5 mM diisopropyl fluorophosphate before hepatic samples of 1 g each were isolated. Each tissue sample was placed in a test tube and subjected to three cycles of freezing (dry ice-acetone bath) and thawing. After adding the same buffer (5 ml) containing an additional 35 mM of β -octyl-glucoside, the hepatic sample was homogenized by a Polytron homogenizer (PT 10-35, Kinematica GmbH Littau, Switzerland) set at full speed with three consecutive 30-sec bursts prior to centrifugation at 48,000 \times g for 20 min at 4°C (Himac CS-120 centrifuge; Hitachi Co. Ltd., Tokyo, Japan). Supernatants were separated from the pellets, and the radioactivity was counted. In a procedure similar to that used on liver tissues, feces were homogenized in the presence of 0.1 M PBS (pH 6.0) before centrifugation at 10,000 \times g for 20 min at 4°C. The liver, feces and urine samples were analyzed by CE and TLC without further treatment. Each sample was also analyzed by both size-exclusion HPLC and reverse-phase HPLC (RP-HPLC) analyses after filtering through a polycarbonate membrane with a diameter of 0.22 μm (Myrex, Millipore Ltd., Tokyo, Japan) and a 10,000-Da cut-off ultrafiltration membrane (Millipore Ltd.), respectively. RP-HPLC analyses (Cosmosil 5C₁₈-AR, 4.6 \times 250 mm, Nacalai Tesque) were eluted with a mixture of methanol and 20% aqueous ammonium acetate (1:10) at a flow rate of 1 ml/min. The radioactivity level in each fraction (1 ml) was then determined with a well counter. Each analysis was also carried out by co-

chromatography with either NH_2 -Bz-EDTA- ^{111}In or lysine-SCN-Bz-EDTA- ^{111}In .

Subcellular distribution of radioactivity in the murine liver was investigated by perfusing the organ *in situ* with cold 0.25 M sucrose buffered with 10 mM phosphate (pH 7.5) at 1 and 3 hr postinjection of NGA-SCN-Bz-EDTA- ^{111}In and 1, 3 and 24 hr postinjection of NMA-SCN-Bz-EDTA- ^{111}In . The liver was treated according to the procedure of Yamada et al. (26) with slight modifications. In brief, the isolated organ was minced with scissors, suspended in fourfold volume of the same buffer prior to homogenization with a Dounce homogenizer by hand (20 strokes). This was followed by two final strokes in an ice-cooled Potter-Elvehjem homogenizer with a Teflon pestle rotated at 800 rpm. The resulting 20% homogenate was centrifuged twice for 5 min at 340 \times g at 4°C. The isolated supernatant was then layered on top of iso-osmotic (0.25 M sucrose) Percoll (Pharmacia Biotech Co. Ltd.) at a density of 1.08 g/ml. After centrifugation at 20,000 \times g (RP 30 rotor; Hitachi Co. Ltd., Tokyo) for 90 min at 4°C, the gradients were collected in 14 fractions before analysis on β -galactosidase activity (27), density and radioactivity counts of the respective fraction.

Radioactive fractions (100 μl each) obtained by Percoll density gradient centrifugation were mixed with 2 ml each of either isotonic 0.25 M sucrose buffered with 10 mM sodium phosphate (pH 7.5) or hypotonic buffer (5 mM sodium phosphate, pH 7.4) with or without an additional β -octyl-glucoside (35 mM). The mixtures were incubated at room temperature for 10 min prior to centrifugation at 320,000 \times g for 1 hr at 4°C. Radioactivity counts of supernatant (500 μl) were determined, assuming the supernatant volume was 2 ml.

RESULTS

Radiochemical yields of labeling SCN-Bz-EDTA- and DTPA-conjugated neoglycoalbumins with ^{111}In exceeded 92% and 83%, respectively. Radiolabeling of NGA- and NMA-SCN-Bz-EDTA with ^{111}In at lower pH was found to be useful to prepare NGA- and NMA-SCN-Bz-EDTA- ^{111}In of higher specific activities in good yields. Radiochemical purities of ^{111}In -labeled NGA and NMA used for *in vivo* studies before and after EDTA chase are shown in Table 1. Radioiodinated NGA and NMA after purification by Sephadex G-50 column chromatography yielded 92% radiochemical purity. Lysine-SCN-Bz-EDTA and NH_2 -Bz-EDTA were chelated with ^{111}In to produce radiochemical yields of more than 98% after 10 min incubation at room temperature when determined by TLC, CE and RP-HPLC analyses.

Collagenase digestion of liver cells indicated more than 85% of the injected radioactivity counts were found in parenchymal and nonparenchymal cells at 15 min after NGA-SCN-Bz-EDTA- ^{111}In and NMA-SCN-Bz-EDTA- ^{111}In injection, respectively.

Radioactivity localization in the liver 10 min after concomitant injections of either NGA- or NMA-SCN-Bz-EDTA- ^{111}In with varying respective amounts of NGA or NMA indicated decreases in radioactivity counts of the ^{111}In -labeled neoglycoalbumins in liver coincided with increasing amounts of NGA and NMA, respectively (Fig. 2). However, in the case of blood, radioactivity counts dis-

TABLE 1
Radiochemical Purities of ^{111}In -Labeled NGA and NMA*

	Before EDTA chase		After EDTA chase [†]			
	EP [‡]	TLC [§]	(5 min)		(60 min)	
			EP [‡]	TLC [§]	EP [‡]	TLC [§]
NGA-SCN-Bz-EDTA- ^{111}In (pH 6.0) [¶]	95.8	95.9	96.4	95.0	94.4	92.9
NGA-SCN-Bz-EDTA- ^{111}In (pH 3.0)**	97.5	97.2	n.d.	n.d.	96.8	95.8
NMA-SCN-Bz-EDTA- ^{111}In (pH 6.0)	99.0	98.6	98.9	98.4	98.9	98.2
NMA-SCN-Bz-EDTA- ^{111}In (pH 3.0)	96.5	95.8	97.1	96.4	97.3	97.1
NGA-DTPA- ^{111}In	83.6	91.7	85.2	89.2	86.0	89.2
NMA-DTPA- ^{111}In	92.0	94.8	92.8	95.0	92.8	94.4

*Expressed as percent radioactivity to protein fraction.

[†]A hundred molar excess of EDTA compared to NGA or NMA was added.

[‡]Radiochemical purities determined by celluloseacetate electrophoresis.

[§]Radiochemical purities determined by thin layer chromatography.

[¶]Radiolabeling carried out in 20 mM MES-buffered saline (pH 6.0).

**Radiolabeling carried out in 0.1 M acetate buffer (pH 3.0).

n.d. = not determined.

played an increase proportional to increases in concomitant administration of NGA and NMA, respectively.

The biodistribution of radioactivity after NGA-SCN-Bz-EDTA- ^{111}In and NMA-SCN-Bz-EDTA- ^{111}In administration in mice is shown in Table 2 and 3, respectively. The former exhibited a rapid and almost quantitative accumulation of radioactivity in the liver at 10 min postinjection, followed by hepatobiliary excretion. No evidence of enterohepatic circulation of the radioactivity was observed. At 24-hr postinjection, 80% and 5% of the injected radioactivity counts of NGA-SCN-Bz-EDTA- ^{111}In were recovered in the feces and urine, respectively. Similarly, NMA-SCN-Bz-EDTA- ^{111}In indicated almost quantitative radioactivity accumulation in the liver, although its accumulation rate was slightly slower than that of NGA-SCN-Bz-EDTA- ^{111}In . As the radioactivity elimination rate of

NMA-SCN-Bz-EDTA- ^{111}In from the liver was much slower than NGA-SCN-Bz-EDTA- ^{111}In , a higher percentage (60%) of the injected radioactivity level remained in the organ coupled with only 26% and 7% of the injected radioactivity counts registered respectively in the urine and feces during this 24-hr interval. When NGA was directly labeled with ^{111}In , all the radioactivity was detected at the origin on CE analysis. Under similar conditions, both NGA- and NMA-SCN-Bz-EDTA- ^{111}In indicated a single peak at 2 cm anode from the origin. When the ^{111}In -NGA via direct labeling was injected in mice, 60% and 71% of the injected radioactivity counts were found in the liver at 10 min and 24 hr postinjection, respectively. During 24-hr postinjection intervals, 2.3% and 1.3% of the radioactivity were recovered in the feces and urine, respectively. Similar results were observed with ^{111}In -labeled NMA.

Comparative distribution of radioactivity with ^{131}I - and ^{111}In -labeled NGA and NMA indicated that NGA-SCN-Bz-EDTA- ^{111}In displayed faster and much delayed radioactivity elimination rates from the liver than those of NGA-DTPA- ^{111}In and NGA- ^{131}I , respectively (Fig. 3). However, NMA-SCN-Bz-EDTA- ^{111}In manifested an elimination rate that was similar to and much slower than those of NMA-DTPA- ^{111}In and NMA- ^{131}I , respectively.

Supernatants of the liver homogenate at 1 hr postinjection of NGA-SCN-Bz-EDTA- ^{111}In and NMA-SCN-Bz-EDTA- ^{111}In was extracted with an efficiency of more than 93%. The size-exclusion HPLC profile of each supernatant depicted a single radioactivity peak at 23 min, a retention time which is representative of small molecular weight compounds such as NH_2 -Bz-EDTA- ^{111}In and lysine-SCN-Bz-EDTA- ^{111}In . Under similar conditions, the parental

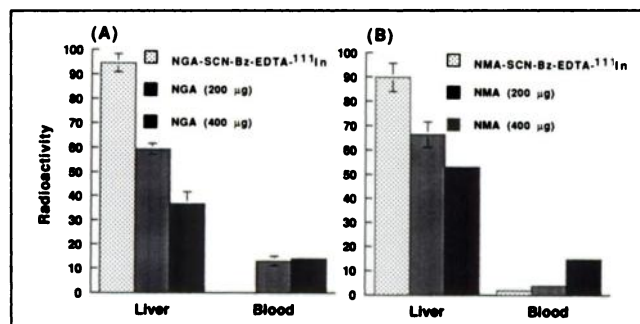


FIGURE 2. Radioactivity in the liver and blood of mice after 10 min intravenous injections of NGA-SCN-Bz-EDTA- ^{111}In (A) and NMA-SCN-Bz-EDTA- ^{111}In (B) with varying amounts of NGA and NMA, respectively. Radioactivity counts in the liver and blood are expressed as %ID and %ID/g, respectively.

TABLE 2
Biodistribution of Radioactivity after Intravenous Injection of NGA-SCN-Bz-EDTA-¹¹¹In in Mice*

Tissue	Percent of injected dose per tissue					
	0.17 hr	0.5 hr	1 hr	3 hr	6 hr	24 hr
Blood†	0.12 (0.06)	0.07 (0.01)	0.08 (0.01)	0.04 (0.01)	0.03 (0.02)	0.01 (0.01)
Liver	94.64 (3.72)	80.05 (4.82)	64.55 (4.16)	36.11 (1.46)	14.73 (2.25)	6.39 (1.28)
Intestine	0.84 (0.34)	14.35 (1.68)	31.04 (7.74)	39.77 (5.79)	25.51 (4.91)	3.54 (1.67)
Kidney	0.16 (0.09)	0.25 (0.12)	0.22 (0.14)	0.12 (0.02)	0.14 (0.05)	0.08 (0.01)
Spleen	0.03 (0.01)	0.03 (0.01)	0.03 (0.01)	0.03 (0.02)	0.02 (0.01)	0.01 (0.01)
Feces						81.08 (6.96)
Urine						5.64 (0.65)

*Each value represents the mean (1 s.d.) for five animals each point.

†Expressed as percent dose per gram.

NGA- and NMA-SCN-Bz-EDTA-¹¹¹In (indicated by dotted line) were eluted at 13 min (Fig. 4A). In RP-HPLC, although the radioactivity was eluted as a single peak at the retention time (8 min) similar to that of lysine-SCN-Bz-EDTA-¹¹¹In, NH₂-Bz-EDTA-¹¹¹In was eluted at a retention time of 5 min (Fig. 4B). CE analyses of each supernatant indicated a single radioactivity peak at 1 cm anode from the origin, which was well correlated to lysine-SCN-Bz-EDTA-¹¹¹In (Fig. 4C). In this analysis, NH₂-Bz-EDTA-¹¹¹In was detected at 3.5 to 4 cm anode from the origin. TLC analyses of the respective supernatants again illustrated a radioactivity peak with a R_f value of 0.6, which was equivalent to that of lysine-SCN-Bz-EDTA-¹¹¹In (Fig. 4D). NH₂-Bz-EDTA-¹¹¹In indicated a single band at the R_f value of 0.4. In each analytical system, all supernatants showed a single radioactivity peak even when cochromatographed with lysine-SCN-Bz-EDTA-¹¹¹In. Similar results were obtained from each chromatographic analysis of liver homogenates obtained at 3 hr postinjection of NGA- and NMA-SCN-Bz-EDTA-¹¹¹In (data not shown).

Chromatographic analyses of feces, liver supernatants and urine samples were performed at 24 hr postinjection of NGA-SCN-Bz-EDTA-¹¹¹In and NMA-SCN-Bz-EDTA-¹¹¹In, respectively (Fig. 5). In each analytical system, all

the samples demonstrated chromatographic behaviors similar to those of liver homogenate at 1 hr postinjection of NGA- and NMA-SCN-Bz-EDTA-¹¹¹In (Fig. 4), except for a second radioactivity peak detected in the RP-HPLC (Fig. 5B) and TLC (Fig. 5D) analyses. The major and minor radioactivities represented about 75% and 20% of each sample. Although some radioactivities were off by a fraction in TLC analyses, cochromatographic analyses confirmed that the behaviors of major and minor radioactivities were well correlated with those of lysine-SCN-Bz-EDTA-¹¹¹In and NH₂-Bz-EDTA-¹¹¹In, respectively.

To further pursue the fate of radiolabeled metabolites after hepatic incorporation, the subcellular distribution of radioactivity of liver homogenates at 1 and 3 hr postinjection of NGA-SCN-Bz-EDTA-¹¹¹In and 1, 3 and 24 hr postinjection of NMA-SCN-Bz-EDTA-¹¹¹In was investigated by Percoll density gradient centrifugation. Every liver homogenate indicated a single radioactivity peak at a density of 1.10 g/ml. This peak correlated well with the β-galactosidase activity profile. The Percoll density gradient centrifugation profile of liver homogenate at 3 hr postinjection of NMA-SCN-Bz-EDTA-¹¹¹In is shown in Figure 6 as a typical example.

TABLE 3
Biodistribution of Radioactivity after Intravenous Injection of NMA-SCN-Bz-EDTA-¹¹¹In in Mice*

Tissue	Percent injected dose per tissue					
	0.17 hr	0.5 hr	1 hr	3 hr	6 hr	24 hr
Blood†	1.93 (0.47)	0.46 (0.13)	0.27 (0.06)	0.14 (0.10)	0.12 (0.01)	0.05 (0.02)
Liver	89.82 (5.81)	95.53 (1.06)	95.72 (2.82)	92.51 (2.31)	85.31 (3.55)	60.95 (3.48)
Intestine	0.70 (0.04)	1.93 (0.10)	0.95 (0.08)	1.61 (0.09)	2.71 (0.16)	1.08 (0.26)
Kidney	0.31 (0.05)	0.31 (0.06)	0.34 (0.02)	0.39 (0.07)	0.41 (0.08)	0.32 (0.06)
Spleen	2.35 (0.45)	2.48 (0.17)	1.96 (0.26)	1.95 (0.24)	1.48 (0.39)	1.12 (0.25)
Feces						7.49 (1.13)
Urine						26.93 (1.61)

*Each value represents the mean (1 s.d.) for five animals each point.

†Expressed as percent injected dose per gram.

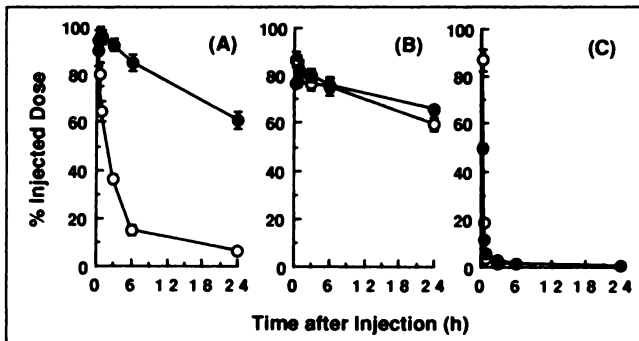


FIGURE 3. Comparative radioactivity clearance from the liver after intravenous injection of NGA (○) and NMA (●) labeled with SCN-Bz-EDTA-¹¹¹In (A), DTPA-¹¹¹In (B), and ¹³¹I (C). NGA-SCN-Bz-EDTA-¹¹¹In showed faster and much slower radioactivity clearance from the liver than NGA-DTPA-¹¹¹In and NGA-¹³¹I, respectively. NMA-SCN-Bz-EDTA-¹¹¹In and NMA-DTPA-¹¹¹In manifested similar radioactivity clearance that was much slower than that of NMA-¹³¹I.

The radioactive fraction from Percoll density gradient centrifugation was then incubated in an isotonic buffer to extract radiolabeled metabolites present on the external lysosomal membrane, whereas a hypotonic buffer with or without surfactant were used to extract radiolabeled metabolites from both external lysosomal membrane and

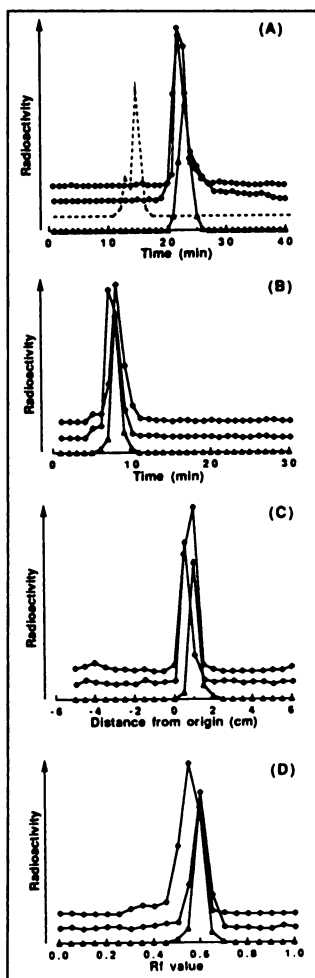


FIGURE 4. Chromatographic analyses of liver homogenates at 1 hr postinjection of NGA-SCN-Bz-EDTA-¹¹¹In (◆) and NMA-SCN-Bz-EDTA-¹¹¹In (◇) using lysine-SCN-Bz-EDTA-¹¹¹In (▲) as a reference. All samples were analyzed by the size-exclusion HPLC (A), RP-HPLC (B), CE (C) and TLC (D).

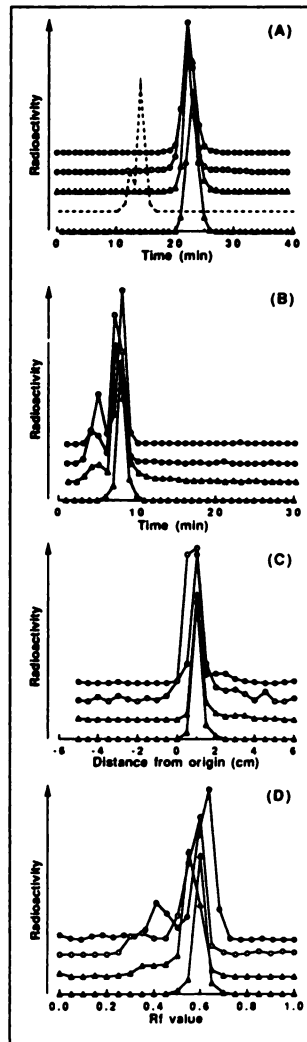


FIGURE 5. Plots of radioactivity counts of feces (●) with intravenous NGA-SCN-Bz-EDTA-¹¹¹In and liver homogenate (○) and urine (△) with intravenous NMA-SCN-Bz-EDTA-¹¹¹In at 24 hr postadministration. Chromatographic behaviors of lysine-SCN-Bz-EDTA-¹¹¹In (▲) were used as the reference. All samples were analyzed by the size-exclusion HPLC (A), RP-HPLC (B), CE (C) and TLC (D). In (B) and (D), NH₂-Bz-EDTA-¹¹¹In indicated a single radioactivity peak at a retention time of 5 min and a Rf value of 0.4, respectively (data not shown).

within the lysosomal lumen (Fig. 7). At 1 hr postinjection, radioactivity counts extracted in the isotonic buffer were approximately half of that in the hypotonic buffers for both NGA- and NMA-SCN-Bz-EDTA-¹¹¹In (Figs. 7A and B). Although only a slight increase of radioactivity counts in the isotonic buffer from 1 to 3 hr postinjection of NGA-SCN-Bz-EDTA-¹¹¹In was registered, the radioactivity increase after NMA-SCN-Bz-EDTA-¹¹¹In administration was evidently observed within the same interval. Radioactivity counts in the isotonic extract approximated to 80% those of the hypotonic extract at 3 and 24 hr postinjection of NMA-SCN-Bz-EDTA-¹¹¹In.

DISCUSSION

Gallium-67- and ^{99m}Tc-labeled NGA are evaluated as potential radiopharmaceuticals for studying hepatic functions (28–31). These radiolabeled NGAs have been shown to accumulate in parenchymal cells of the liver via the receptor-mediated endocytosis. In this study, specific radioactivity accumulation in parenchymal and nonparenchymal cells of murine liver was demonstrated after NGA-SCN-Bz-EDTA-¹¹¹In and NMA-SCN-Bz-EDTA-¹¹¹In

administrations, followed by collagenase perfusion. Accumulation of NGA- and NMA-SCN-Bz-EDTA-¹¹¹In in the liver was also inhibited in a dose-dependent fashion by the presence of NGA and NMA, respectively (Fig. 2). These results indicated that both NGA-SCN-Bz-EDTA-¹¹¹In and NMA-SCN-Bz-EDTA-¹¹¹In used in this study were incorporated by parenchymal and nonparenchymal cells of the liver via the receptor-mediated endocytosis. In addition, since the radiochemical purities of NGA-SCN-Bz-EDTA-¹¹¹In and NMA-SCN-Bz-EDTA-¹¹¹In were unchanged before and after EDTA chase (Table 1), the radioactivities of NGA- and NMA-SCN-Bz-EDTA-¹¹¹In were probably chelated with the Bz-EDTA moiety. Similar results were observed with NMA-DTPA-¹¹¹In. Therefore, *in vivo* behaviors of radioactivity of the three proteins would reflect the fate of radiolabels after lysosomal proteolysis in parenchymal and nonparenchymal cells of the liver.

An attempt to remove nonspecifically bound ¹¹¹In of NGA-DTPA-¹¹¹In by Sephadex G-50 column chromatography following EDTA chase did not enhance the radiochemical purity when determined by CE analysis. Considering the high and prolonged hepatic radioactivity of ¹¹¹In-NGA produced by direct labeling, the radioactivity localization of NGA-DTPA-¹¹¹In was overestimated. Even when the effect of nonchelated ¹¹¹In radioactivity was subtracted, NGA-DTPA-¹¹¹In indicated high and persistent radioactivity in the liver (Fig. 3). This finding coincided well with data presented recently by Duncan and Welch utilizing a similar series of experiments (32).

NGA-SCN-Bz-EDTA-¹¹¹In manifested a gradual elimination of radioactivity from the liver to feces with more than 80% of the injected radioactivity recovered in the feces at 24 hr postinjection (Table 2). Analyses of the radiolabeled metabolites excreted in feces indicated that the major radiolabeled metabolite (ca. 75% of the feces) coincided with chromatographic behaviors of lysine-SCN-Bz-EDTA-¹¹¹In (Fig. 5). RP-HPLC and TLC analyses of the feces further suggested that the metabolite with a minor radioactivity (ca. 20% of the feces) was likely to be to NH₂-Bz-EDTA-¹¹¹In, which is a potential product after hydrolysis of the thiourea bond of lysine-SCN-Bz-EDTA-¹¹¹In (33) and might be generated in the liver and intestine.

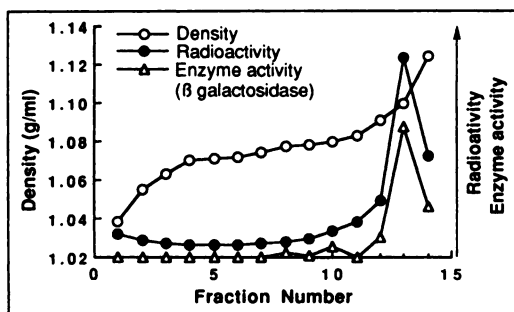


FIGURE 6. Percoll density gradient profiles of liver homogenate at 3 hr postinjection of NMA-SCN-Bz-EDTA-¹¹¹In. A single radioactivity peak (●) that coincided with β -galactosidase activity (Δ) was detected at a density (○) of ca. 1.10 g/ml.

However, NMA-SCN-Bz-EDTA-¹¹¹In demonstrated persistent radioactivity localization in the liver and the radiolabeled metabolites were mainly excreted in the urine (Table 3). Analyses of radiolabeled metabolites in the liver and urine at 24 hr postinjection of NMA-SCN-Bz-EDTA-¹¹¹In indicated results similar to those of NGA-SCN-Bz-EDTA-¹¹¹In (Fig. 5).

Furthermore, similar analyses conducted on the liver homogenates at 1 hr postinjection of NGA- and NMA-SCN-Bz-EDTA-¹¹¹In revealed that the metabolite displayed chromatographic behaviors similar to those of lysine-SCN-Bz-EDTA-¹¹¹In (Fig. 4). As such, when SCN-Bz-EDTA was used as a BCA to label neoglycoalbumins with ¹¹¹In, the major radiolabeled metabolite after lysosomal proteolysis in both parenchymal and nonparenchymal cells of the liver was identical and most likely to be lysine-SCN-Bz-EDTA-¹¹¹In, where all peptide bonds of the HSA backbone were cleaved. Although this metabolite was generated and represented all the radioactivity retained in the liver as early as 1 hr after administration (Fig. 4), 65% and 95% of the injected radioactivity counts remained in parenchymal and nonparenchymal cells of the liver, respectively at this postinjection time (Table 2 and 3). Since less than 5% of the injected radioactivity was detected in both liver cell types 1 hr postinjection of radioiodinated NGA and NMA (Fig. 3), the slow excretion rate of the radiolabeled metabolites derived from SCN-Bz-EDTA-¹¹¹In was responsible for the delayed radioactivity elimination from both liver cell types.

To investigate the slow excretion rate of the radiolabeled metabolites from each liver cell type, the subcellular distribution of radioactivity was investigated. At 1 and 3 hr postinjection of NGA-SCN-Bz-EDTA-¹¹¹In and at 1, 3 and 24 hr postinjection of NMA-SCN-Bz-EDTA-¹¹¹In, when all the radioactivity remained in each liver cell type was present as the final metabolites, all radioactivity counts were detected in the lysosomal fraction without intracellular transport to other organelles and interaction with biomolecules in the cytoplasm (Fig. 6). This demonstrates that the elimination rate of radiolabeled metabolites from the lysosome plays a critical role in the radioactivity excretion from both liver cell types.

For further pursuit of behaviors of the radiolabeled metabolites in lysosomes, the lysosomal fraction was treated with isotonic or hypotonic buffer to extract the radioactivity associated with external lysosomal membrane or both external and internal lysosomal fractions, respectively. Isotonic treatment of lysosome at 1 hr postinjection of both NGA- and NMA-SCN-Bz-EDTA-¹¹¹In suggests that one-half of the radioactivity counts in the lysosome was present within the lysosomal lumen, whereas the other half was associated with the external lysosomal membrane (Fig. 7).

Since both ¹³¹I-labeled NGA and NMA exhibited much less radioactivity in both cell types of the liver at the same postinjection interval (Fig. 3), both permeation rate through the lysosome membrane and elimination rate from the external lysosomal membrane of the ¹¹¹In-labeled me-

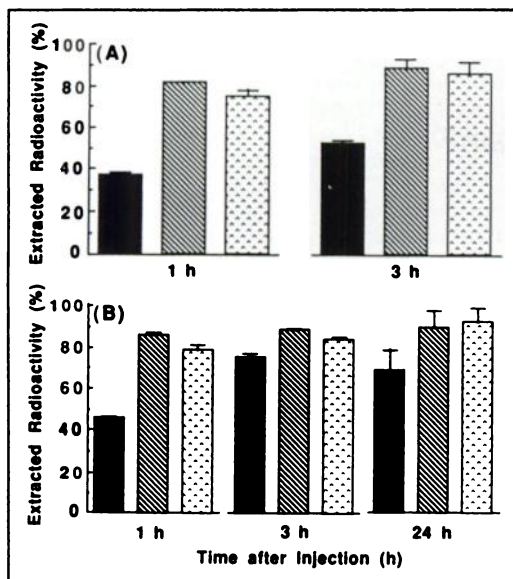


FIGURE 7. Percent radioactivity extracted in the supernatant after incubating the radioactive fraction of the Percoll density gradient obtained at 1 and 3 hr postinjection of NGA-SCN-Bz-EDTA-¹¹¹In (A) as well as 1, 3, and 24 hr postinjection of NMA-SCN-Bz-EDTA-¹¹¹In (B) with isotonic (solid column), hypotonic (hatched column) and hypotonic buffers containing a surfactant (35 mM β -octyl-glucoside) (dotted column).

tabolites contributed to the slow elimination from both cell types of the liver. Furthermore, although most of the radioactivity was present in the external lysosome membrane, high radioactivity counts were still detected in the liver at 3 and 24 hr postinjection of NMA-SCN-Bz-EDTA-¹¹¹In (Table 3 and Fig. 7). This was in contrast to NGA-SCN-Bz-EDTA-¹¹¹In at 3 hr postinjection (Table 2 and Fig. 7). These results indicated that most of the radiolabeled metabolites had passed through the lysosomal membrane extracellularly but was still associated with the external lysosomal membrane at 3 hr postinjection of NMA-SCN-Bz-EDTA-¹¹¹In.

In summary, the slower radioactivity elimination rate of NGA- and NMA-SCN-Bz-EDTA-¹¹¹In from liver compared to those of radioiodinated proteins after injection was probably attributed to not only the slower permeation rate of the ¹¹¹In-labeled metabolites from lysosomal membrane but also slower excretion rate from the external lysosomal membrane. The latter contributed more critically to elimination from nonparenchymal cells. This disparity may be due to the biliary excretion characteristics of the ¹¹¹In-labeled metabolites and the bile secretion mechanism of parenchymal cells of the liver.

In this study, NGA and NMA were used as carrier proteins to investigate the fate of radiolabels derived from SCN-Bz-EDTA-¹¹¹In after lysosomal proteolysis in different cell types of the liver. Despite that SCN-Bz-EDTA covalently links to ϵ -amine groups of lysine residue of proteins, the major radiolabeled metabolite of both NGA and NMA in the liver manifested a single component that correlated with lysine-SCN-Bz-EDTA-¹¹¹In (Fig. 4 and 5),

where all peptide bonds in these proteins were cleaved. Since SCN-Bz-EDTA is conjugated to Mabs via similar conjugation chemistry, similar radiolabeled metabolites may be generated after lysosomal proteolysis of ¹¹¹In-labeled Mabs in both parenchymal and nonparenchymal cells of the liver. Therefore, once Mab-SCN-Bz-EDTA-¹¹¹In was incorporated by the liver via some unknown mechanisms, ¹¹¹In-labeled Mabs would be metabolized and the radiolabeled metabolites would be gradually excreted from the parenchymal cells via hepatobiliary excretion, whereas in the nonparenchymal cells the metabolites would be retained for a longer interval.

Using a similar approach, a recent study has indicated that when DTPA is used as a BCA for both NGA and NMA, lysine-DTPA-¹¹¹In appears to be the final radiolabeled metabolite in both cell types of the liver. This metabolite indicated persistent retention in both these cell types (32). Similar findings in this study reinforced such observations (Fig. 3). Since parenchymal cells have been reported to be the common site where antibodies in the murine liver are located (34,35), a difference in the elimination rate of NGA-SCN-Bz-EDTA-¹¹¹In and NGA-DTPA-¹¹¹In from the parenchymal cell may account for the lower ¹¹¹In radioactivity of Mab-SCN-Bz-EDTA-¹¹¹In in the murine liver compared to Mab-DTPA-¹¹¹In.

In conclusion, the use of NGA and NMA as carrier proteins rendered detailed information as to the fate of radioactivity after lysosomal proteolysis in parenchymal and nonparenchymal cells of the liver. Coupled with biodistribution studies in tumor-bearing athymic mice using Mabs, this method presented detailed and reliable evaluations of the practical use of newly designed BCAs for Mabs as well as other proteins and peptides. Discrepancies between animal and clinical studies with the use of various radioimmunoconjugates may also be accounted for by this method.

ACKNOWLEDGMENTS

The authors thank Nihon Medi-Physics Co. Ltd., Takarazuka, Japan, and Daiichi Radioisotope Labs. Ltd., Tokyo for their kind gifts of ¹¹¹InCl₃ and Na¹³¹I, respectively. This work was supported in part by a Grant-in-Aid for Developing Scientific Research (# 05151036) from the Ministry of Education, Science and Culture of Japan. Part of this work was presented at the Society of Nuclear Medicine's 40th Annual Meeting in Toronto, Ontario, June 1993.

REFERENCES

- Brechbiel MW, Gansow OA, Atcher RW, et al. Synthesis of 1-(p-isothiocyanatobenzyl) derivatives of DTPA and EDTA. Antibody labeling and tumor-imaging study. *Inorg Chem* 1986;25:2772-2781.
- Craig AS, Helps IM, Jankowski KJ, et al. Towards tumour imaging with Indium-111-labelled macrocycle-antibody conjugates. *J Chem Soc Chem Commun* 1989;794-796.
- Deshpande SV, Subramanian R, McCall MJ, DeNardo SJ, DeNardo GL, Mearns CF. Metabolism of indium chelates attached to monoclonal antibody: minimal transchelation of indium from benzyl-EDTA chelate in vivo. *J Nucl Med* 1990;31:218-224.
- Schwarz SW, Mathias CJ, Sun JY, et al. Evaluation of two new bifunctional

- chelates for radiolabeling a parathyroid-specific monoclonal antibody with In-111. *Nucl Med Biol* 1991;18:477-481.
5. Subramanian R, Colony J, Shaban S, et al. New chelating agent for attaching indium-111 to monoclonal antibodies—in vitro and in vivo evaluation. *Bioconj Chem* 1992;3:248-255.
 6. Yokoyama K, Carrasquillo JA, Chang A, et al. Differences in biodistribution of indium-111- and iodine-131-labeled B72.3 monoclonal antibodies in patients with colorectal cancer. *J Nucl Med* 1989;30:320-327.
 7. Himmelsbach M, Wahl RL. Studies on the metabolic fate of ¹¹¹In-labeled Antibodies. *Nucl Med Biol* 1989;16:839-845.
 8. Motta-Hennessy C, Sharkey RM, Goldenberg DM. Metabolism of indium-111-labeled murine monoclonal antibody in tumor and normal tissue of the athymic mouse. *J Nucl Med* 1990;31:1510-1519.
 9. Paik CH, Sood VK, Le N, et al. Radiolabeled products in rat liver and serum after administration of antibody-amide-DTPA-indium-111. *Nucl Med Biol* 1992;19:517-522.
 10. Alberts B, Bray D, Lewis J, Raff M, Roberts K, Watson JD. Membrane transport of macromolecules and particles; exocytosis and endocytosis. In: *Molecular biology of the cell*. New York: Garland Publishing Inc.; 1983; 302-317.
 11. Santoro L, Rebut A, Journet AM, Colomb MG. Major involvement of cathepsin B in the intracellular proteolytic processing of endogenous IgGs in U937 cells. *Mol Immunol* 1993;30:1033-1039.
 12. Geissler F, Anderson SK, Venkatesan P, Press O. Intracellular catabolism of radiolabeled anti- μ antibodies by malignant C-cells. *Cancer Res* 1992;52:2907-2915.
 13. Ashwell G, Harford J. Carbohydrate-specific receptors of the liver. *Ann Rev Biochem* 1982;51:531-554.
 14. Stockert RJ, Morell AG. Hepatic binding protein: the galactose-specific receptor of mammalian hepatocytes. *Hepatology* 1983;3:750-757.
 15. Hubbard AL, Wilson G, Ashwell G, Stukenbrok H. An electron microscope autoradiographic study of the carbohydrate recognition systems in rat liver. *J Cell Biol* 1979;83:47-64.
 16. Shen TY. Drug delivery via cell-surface receptors. In: Borchardt RT, Repta AJ, Stella VJ, eds. *Directed drug delivery*. Clifton: Humana Press; 1985; 231-245.
 17. Meares CF, McCall MJ, Reardan DT, Goodwin DA, Diamanti CI, McTigue M. Conjugation of antibodies with bifunctional chelating agents: isothiocyanate and bromoacetamide reagents, methods of analysis, and subsequent addition to metal ions. *Anal Biochem* 1984;142:68-78.
 18. Lee YC, Stowell CP, Krantz MJ. 2-Imino-2-methoxyethyl 1-thioglycosides: new reagents for attaching sugars to proteins. *Biochemistry* 1976;15:3956-3963.
 19. Stowell CP, Lee YC. Preparation of some new neoglycoproteins by amidination of bovine serum albumin using 2-imino-2-methoxyethyl 1-thioglycosides. *Biochemistry* 1980;19:4899-4904.
 20. Snyder SL, Sobocinski PZ. An improved 2,4,6-trinitrobenzenesulfonic acid method for the determination of amines. *Anal Biochem* 1975;54:284-288.
 21. Wilbur DS, Hadley SW, Grant LM, Hylarides MD. Radioiodinated iodobenzoyl conjugates of a monoclonal antibody Fab fragment. In vivo comparisons with chloramine-T-labeled Fab. *Bioconj Chem* 1991;2:111-116.
 22. Imai S, Morimoto J, Tsubura T, et al. Genetic marker patterns and endogenous mammary tumor virus genes in inbred mouse strains in Japan. *Exp Anim* 1986;35:263-273.
 23. Seglen PO. Preparation of rat liver cells. *Exp Cell Res* 1973;76:25-30.
 24. Arano Y, Matsushima H, Tagawa M, et al. A new design of radioimmunoconjugate releasing hippurate-like radiometal chelate for tumor-selective radioactivity delivery. *Nucl Med Biol* 1994;21:63-69.
 25. Arano Y, Inoue T, Mukai T, et al. Discriminated release of a hippurate-like radiometal chelate in nontarget tissues for target selective radioactivity localization using pH-dependent dissociation of reduced antibody. *J Nucl Med* 1994;35:326-333.
 26. Yamada H, Hayashi H, Natori Y. A simple procedure for the isolation of highly purified lysosomes from normal rat liver. *J Biochem* 1984;95:1155-1160.
 27. Wallner SJ, Walker JE. Glycosidases in cell wall-degrading extracts of ripening tomato fruits. *Plant Physiol* 1975;55:94-98.
 28. Koizumi K, Uchiyama G, Arai T, Ainoda T, Yoda Y. A new liver function study using Tc-99m DTPA-galactosyl human serum albumin: evaluation of the validity of several functional parameters. *Ann Nucl Med* 1992;6:83-86.
 29. Stadalnik RC, Vera DR, Woodle E, et al. Technetium-99m NGA functional hepatic imaging: preliminary clinical experience. *J Nucl Med* 1985;26:1233-1242.
 30. Vera DR. Gallium-labeled deferoxamine-galactosyl-neoglycoalbumin: a radiopharmaceutical for regional measurement of hepatic receptor biochemistry. *J Nucl Med* 1992;33:1160-1166.
 31. Vera DR, Krohn KA, Stadalnik RC, Scheibe PO. Tc-99m-galactosyl-neoglycoalbumin: in vitro characterization of receptor-mediated binding. *J Nucl Med* 1984;25:779-787.
 32. Duncan JR, Welch MJ. Intracellular metabolism of indium-111-DTPA-labeled receptor targeted proteins. *J Nucl Med* 1993;34:1728-1738.
 33. Assony SJ. The chemistry of isothiocyanates. In: N Kharasch, eds. *Organic sulfur compounds*. New York: Pergamon Press; 1961:326-338.
 34. Boyle CC, Paine AJ, Mather SJ. The mechanism of hepatic uptake of a radiolabelled monoclonal antibody. *Int J Cancer* 1992;50:912-917.
 35. Sands H, Jones PL. Methods for the study of the metabolism of radiolabeled monoclonal antibodies by liver and tumor. *J Nucl Med* 1987;28:390-398.